




Experimental investigation of the effect of damping coefficients on spring diameter thickness

K.J. Kadhim

Al-Mussaib Technical Institute, Al-Furat Al-Awsat Technical University, 51009 Babylon, Iraq

Corresponding e-mail address: inm.kml@atu.edu.iq

ORCID identifier:  <https://orcid.org/0000-0001-5802-4839>

ABSTRACT

Purpose: The main objective of this research is to study the effect of damping coefficients on the damping strength of shock absorbers using Taguchi Design Experiment (DOE) and rough surface method in Design Expert 7.0.0.

Design/methodology/approach: To achieve and measure the damping force based on the data analysis in the design program. The effecting parameters are: damping diameter (A), gas pressure nitrogen in damping (B), and suspension velocity(C). Consequently, the experiment was carried out in the lab to measure the damping force based on the data analysis.

Findings: The experimental results demonstrated that nitrogen gas at a pressure of 40 bars is appropriate for dealing with motorcycles and that optimum parameter values may be achieved using ANOVA (Analysis of Variance), regression analysis, and confirmation studies.

Research limitations/implications: The measure of the damping force in this process widely depend on the technical specifications of a testing machine. Consequently, machine operating parameters consider the main limiting factor in this process.

Practical implications: In this current work, a steel spring of (50) mm diameter has been used in this experimental investigation to measure the influence of the damping force based on the data analysis. In addition, optimal working parameter values that maximize the performance were identified. The experimental test was planned and conducted according to the ANOVA (Analysis of Variance).

Originality/value: The validation of experimental results shows that this analysis gives an average error 5%, it's also concluded that the gas at a pressure of 40 bars is appropriate for dealing with motorcycles and can be adopted safely.

Keywords: Process parameter, RSM analysis, Damping force, Test machine

Reference to this paper should be given in the following way:

K.J. Kadhim, Experimental investigation of the effect of damping coefficients on spring diameter thickness, Journal of Achievements in Materials and Manufacturing Engineering 115/1 (2022) 16-25. DOI: <https://doi.org/10.5604/01.3001.0016.2338>



PROPERTIES

1. Introduction

Having necessary programs that help analyze the results during operations is essential; therefore, advanced Design of Experiments (DOE) features is required to improve testing methods. Because of this, the factors can be screened to see which ones are significant for explaining process variation. Minitab can assist you in understanding how components interact and drive your process once you've screened them. It can then find the factor settings that produce optimal process performance. The rails are made the bearings, whether they contain gas or liquid, and the brackets, associated with them support the wheels and helical spirals and according to the number of languages and their diameter, as well as the shock absorbers, all of these are links to complete the design of the wheel according to the required design. The main components of the suspension system are divided into links, and deputies and shock absorbers. The importance of damping springs is mainly to reduce vibrations resulting from bumps and potholes in the roads. The suspension system of the front wheels of the motorcycle contains parallel hydraulic forks that extend along the front wheel and point down in the front direction, resulting in a bend in the suspension forks the shock absorbers mentioned above occur with the motorcycle brackets in a vertical position resting on a fixed horizontal surface. Experiments can be repeated several times in the laboratory to easily reach the desired goal, and this is better than real driving on the road. While lab inspections were low cost and can be performed more quickly [1-9]. The model to be optimized the shock absorber is one of the Model's most nonlinear and complex elements. In fact, the shock absorbing force is the effective non-linear effect depending on the piston speed, and is asymmetric against the velocity (compression and rebound) [3-5]. The contents of the basic fork are a telescopically mounted upper tube inside a lower tube containing an oil body, and each tube contains continuous cylindrical surfaces in a sliding connection and is lubricated by a body with a reservoir of oil stored inside the tube. As for the bridge installed on the upper parts of the above-mentioned upper tubes, it is installed on the front wheel with a spindle on the lower tubes. It means that it gives a constant torque on the lower tubes being investigated according to the load and balance data while riding the bike [6-10]. The elastic means extending between the bridge include the source of our research above and the torque force to reach the anti-bending moment of the aforementioned prongs and the impedance of the first bending moment shown above, and we get from this to reduce the sliding friction. There are three basic types of suspension and links in the bars, brackets that support the wheels, coils and shock absorbers. Spirals with shock absorbers reduce the severity of the car during

the loads resulting from large and small bumps and pits of all kinds. The researchers [6-9] referred to the method of analyzing the main components in the suspension process and through the suspension of a group of the front wheels of a motorcycle consisting of hydraulic telescopic parallel forks that extend along the front wheel and tend downward in the forward direction, resulting in a momentary bend in the aforementioned forks with the motorcycle supports in the vertical position on the horizontal surface [11-16]. The extra weight on the front fork affects the wheels by repelling violent shocks when driving on rough and unpaved roads. We search and focus to get the maximum damping power by setting the best individual factors and the optimal quality through design and analysis in the Taguchi system of this experiment, and we note the individual factors in the quality characteristics using the same analytical program above [17-20].

2. Materials and methods

The front suspension is normally incorporated into the front fork. It can be made up with reference to an object made of concentric tubular parts, tubes get the best deals on called motorcycle fork extension tubes that include the hang up inside or multi-rod connection that stores the hanging outside. All other variables were held constant during the experiment. The level of fluid inside the cylinder between the fork and the tube and other attachments connected to the external bearing system is the same as the suspension system mentioned above as parameter constants.

Investigation of affairs experimental conditions. The testing forces for the damping system were on a servo hydraulic experimental detail of the trials – three input control, three levels of factors. Table 1 shows the details of the parameters and their levels of utilization.

Table 1.

Process parameters and levels

A	N ₂ Pressure	30	35	40
B	Velocity, m/s	0.7	0.8	0.1
C	Damping dia, mm	1	1.6	1.9

3. Motorcycle suspension explained

Motorcycles are consisting of many different and connected part which is more complex, and well-engineered by the day, and knowing how it works system the suspension on a motorcycle be a difficult process. For all that understanding belonging to motorcycle comment preparation, how it affects your riding, and what adjustments you can make is a huge benefit. A properly set up suspension will provide you with more comfort and

control. Due to road conditions, the spring supported the motorcycle's body and acted as a vibration absorber. The damper cooperates with the spring to provide a comfortable and safe ride. The damper acts as a dissipate, and the damper function work to reduce the rate of pressure together as it pressed, which is known as compression damping. When a spring is compressed, it must return to its previous shape and dimensions, which is all rebound damping. So, for the motorcycle hang to perform properly, together the spring and the damper overlooked not must be balanced both. The spring controls the bike's mass, whereas the damping affects how fast the spring moves. [19-24]. In Figure 1 the name of the device used for that purpose, and we note the stages of testing the model in the laboratory.

The objective of rebound damping is to properly manage the shock's extension after it has been compressed by lowering the energy within the spring. Through the pressure of the spring, it pushes with great force and clearly when is releasing the pressure. Also, if this system is not controlled, the wheel remains in a continuous rebound state until its oscillating movement is stopped naturally, which takes some time and the experiment is somewhat unsuccessful. Motorcycles are constructed through a hang geometry that includes thorn angle and altitude. Mutable components of a motorbike's suspension geometry might change the geometry; consequently, the front and rear end of the motorcycle should be in sync with each other. The best

results may be reached while the rear shock absorber and front components work together appropriately.

4. Design of motorcycle shock absorbers

Motorcycles under the pressure gas or fluid are compressed shock absorber by gas or liquid, and the gas or liquid is separated from the piston at the toping of the shock absorbers. These parts are installed apps directly or kept in a separate tank. There is another type of shock absorber found in motorcycles in which everything fits in the main cylinder tube. This tube is also called as an internal gas reservoir. Nitrogen is used for making the pressurization of the fluid. Compressed Nitrogen gas is often used as a liquid. To fill the upper tank cavity with pressurized liquid nitrogen, which works excellently in mitigating shock absorption, and reducing the temperature of the liquid in the external tanks, which growths the service life of both gas and liquid together or individually. As indicated in Figure 2 in (A, B, C), A: Working for the aggregation and connected with the liquid nitrogen system (made by distilling liquid air boils at 77.4 Kelvins (-195.8°C) and is used as a coolant) which is used for making the pressurization of the fluid. B as for symmetrical spring damping of a certain number and thickness of (7 mm dia) and C, The lower and upper bushings can be viewed through the telescopic fork and see spring system only.

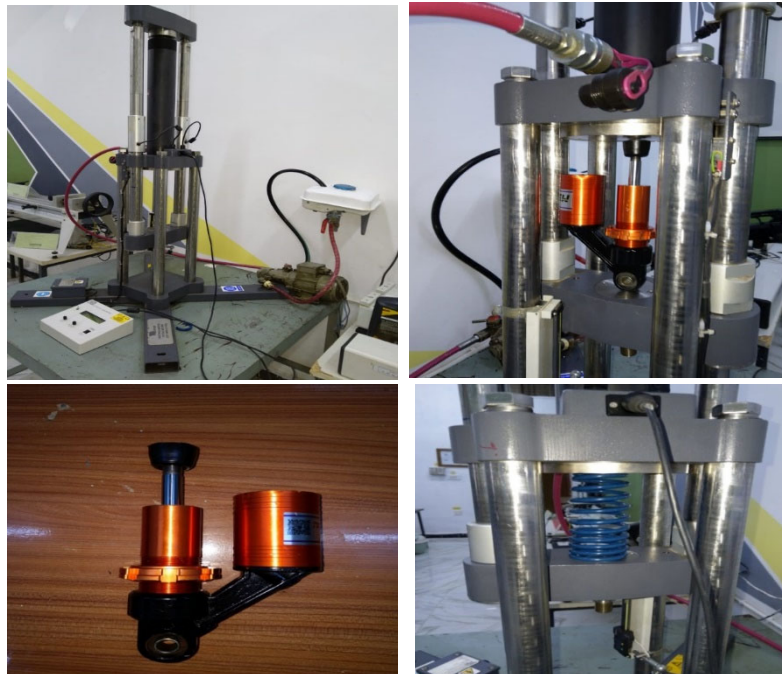


Fig. 1. SM100 Universal material test machine CAP (100KN 10 TON)

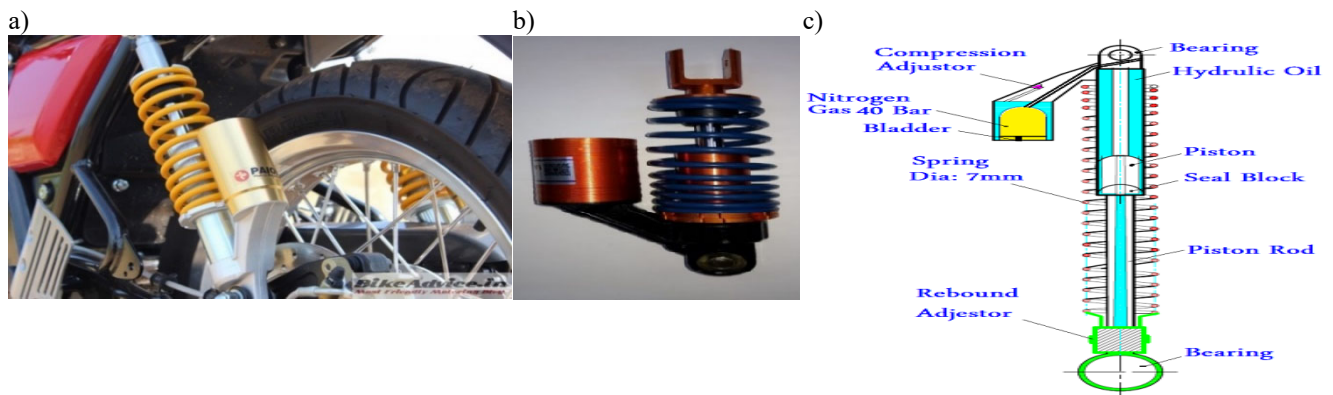


Fig. 2. Parts of the systems

Temperature compensation is built into the motorcycle shock absorbers (not taking temperature during the shock absorbers of the motorcycle in the testing). As the fluid temperature rises, the fluid begins to flow more freely, but this flow is restricted inside the absorbers. As a result, the effect of shock absorption is temperature-independent. Individual rebounding and compression damping adjustments are possible in some modern motorbike shock absorbers. The motorbike shock absorbers also have an adjustable mechanical or hydraulic pre-loading system.

5. Fluid flow in motorcycle shock absorbers

The fluid from the shock absorbers is slowly injected via the needle valves. It can also be injected through various holes in the piston. The shims control the fluid flow. Steel washers serve as shims. The shims are displaced from their original position by the high pressure of the fluid flow. Change the thickness, quantity, or the diameter of the shims to change the damping action's characteristics. The liquid begins to pass into in the piston road during the needle valves (combination of return valves and compression valves) when the shock absorbers of motorbikes are compressed owing to the movement of the motorcycles. The needle valves are insufficient to allow the fluid to flow during rapid compression when the piston's Velocity is high. The fluid begins to flow through the shims located just beneath the piston in this case. The fluid is pushed into an external fluid chamber and displaced by the piston rod. A separate compressive valve forces the fluid into the exterior fluid chamber. This valve is coupled to shims that open when the high piston velocity.

6. Experiments interpreting the results

Data-driven design detail metrics, Central Composite Design: Factors: 3, Replicates: 1, Factorial: One-level: Axial

points 6, Center points in axial 2, and Alpha 1.633. Full factorial and Cube points: 8, Center point in the cube: 4, Axial points 6, Center points in axial 2, and Alpha 1.633. In addition, there are 20 base runs, 20 total runs, and one base block for a central composite design with three elements that will be run in one block. See Central composite designs for rotatable and orthogonally blocked designs. It experimented with different settings for each of the design points' factors. Use the order indicated to determine the conditions for each run while experimenting. Set the N_2 gas pressure (A) to 40 bars (1 = high), the velocity (B) to 2 m/s (1 = high), and the catalyst (C) to 7 Dia (1 = high) in the first run of the experiment.

Quadratic Model evaluation of Response Surface into Design Matrix, Figure 3, Table 2 and No aliases discovered for Quadratic Model Aliases are generated depending on the working response choices, with missing data points taken into account.

A minimum of three df for lack of fit and four df for pure error is recommended. This verifies that the lack of fit test is valid. As seen in Table 2, a test with less df may not discover a lack of fit.

Within each type of coefficient, standard errors should be similar. The ideal VIF value is 1.0. Smaller is preferable; greater than ten, cause concern, indicating that factors are estimated incorrectly cause to multicollinearity. R-squared should be 0.0. Ri-squared should be 0.0. High Ri-squared suggests words are highly linked, which lead to bad models.

The force must be around 80% of the impact which is want to disclose. Make certain the Model (in the previous screen) is set to evaluate the conditions of the experiment think will be meaningful. For leverages near 1.0, this is a requirement in the design analysis. Consider duplicating these points or ensuring they are carried out with extreme caution, as shown in Figure 4.

7. Analyses process

The upper bound of the higher-order matrix is defined in the Table 3 and Figure 4.

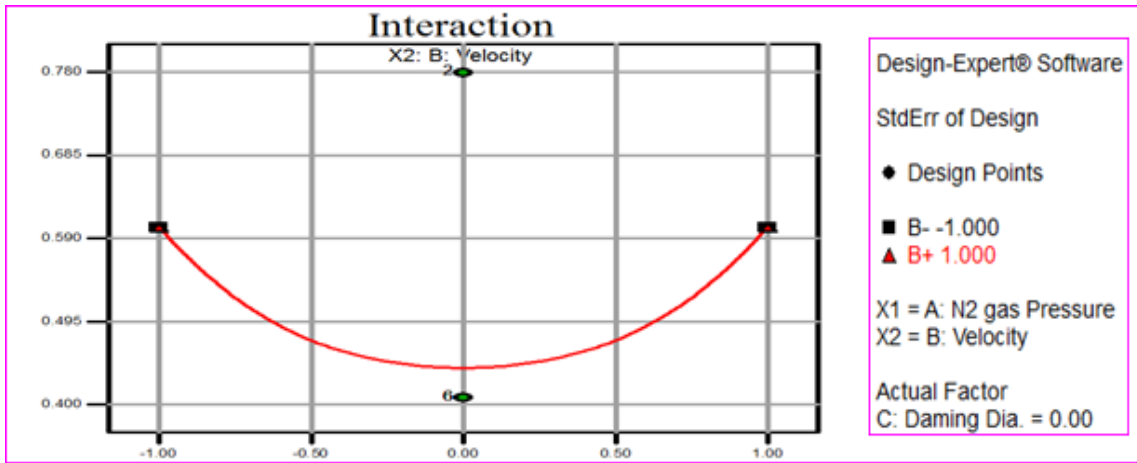


Fig. 3. X1:A: N2:Gas Pressure and X2:B: Velocity VS StdErr of design

Table 2.

Design summary

Factor	Name	Units	Type	Low actual	High actual	Low coded	High coded	Mean	Std. Dev.	
A	N2 gas Pressure	Bar	Numeric	-1.00	1.00	-1.000	1.000	0.000	0.826	
B	Velocity	m/s	Numeric	-1.00	1.00	-1.000	1.000	0.000	0.826	
C	Damping Dia.	mm	Numeric	-1.00	1.00	-1.000	1.000	0.000	0.826	
Response Name	Units	Obs	Analysis	Minimum	Maximum	Mean	Std. Dev.	Ratio		
Y1	Force	N	20	Polynomial	21.00	40.00	27.45	4.72	1.90	Trans Model

Table 3.

Sum of squares serial model [Type I]

Sum of Source Squares	df	Mean Square	F-value	p-value : Prob > F	
Mean vs Total: 15070.05	1	15070.05			<u>Suggested</u>
Linear v: 55.11	3	18.37	0.75	0.5360	
2FI vs L: 44.50	3	14.83	0.56	0.6517	
Quadratic: 114.11	3	38.04	1.64	0.2410	<u>Suggested</u>
Cubic vs 96.39	4	24.10	1.07	0.4463	Aliased
Residual: 134.84	6	22.47			
Total: 15515.00	20	775.75			

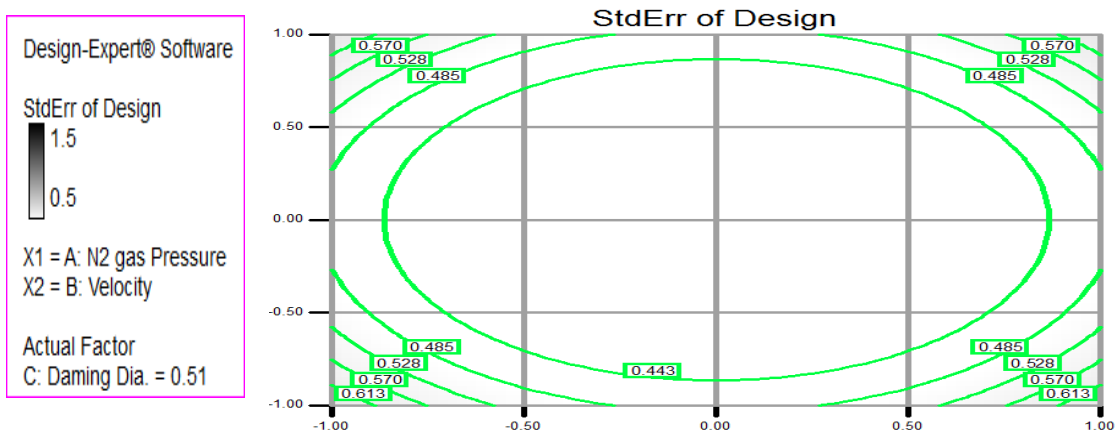


Fig. 4. X1: A: N2 gas pressure VS X2: B: Velocity

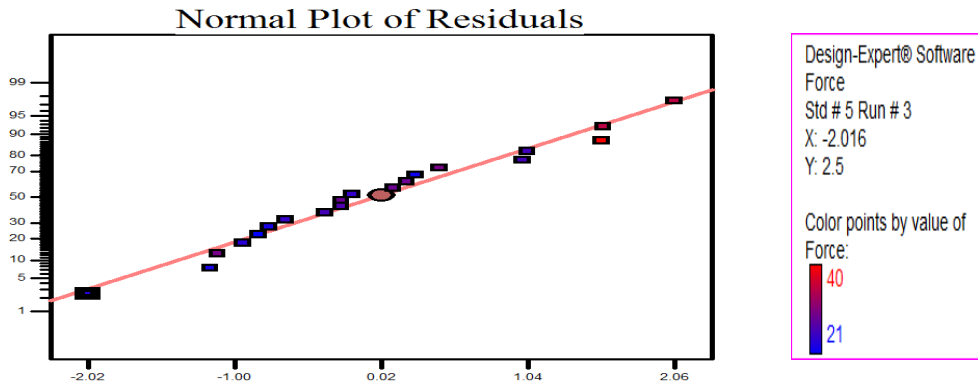


Fig. 5. X: Internally Studentized Residuals VS Y: Normal % Probability

Table 4.

"Model Summary Statistics": we focused on the model that achieves us to increase the size. "Adjusted R-Squared" and the "R-Squared" predicted

	Std.	Adjusted	Predicted			
Source	Dev. R-Squared	R-Squared	R-Squared	R- Squared	PRESS	
Linear	4.94	0.1239	-0.0404	-0.4484	644.45	
2FI	5.15	0.2239	-0.1344	-1.1533	958.10	
<u>Quadratic</u>	<u>4.81</u>	<u>0.4803</u>	<u>0.0126</u>	<u>-1.6309</u>	<u>1170.62</u>	<u>Suggested</u>
Cubic	4.74	0.6969	0.0403	-18.5538	8700.44	Aliased

Table 5.

The strength of the response of the quadratic model on the surface and the analysis of variance (ANOVA)

Source	Sum of squares	df	Mean square	F value	p-value Prob > F
Model	213.72	9	23.75	1.03	0.4795
A-N2 gas Pressure	37.07	1	37.07	1.60	0.2342
B-Velocity	14.73	1	14.73	0.64	0.4434
C-Damping Dia.	3.31	1	3.31	0.14	0.7129
AB	18.00	1	18.00	0.78	0.3983
AC	24.50	1	24.50	1.06	0.3276
BC	2.00	1	2.00	0.086	0.7747
A ²	35.17	1	35.17	1.52	0.2457
B ²	2.11	1	2.11	0.091	0.7689
C ²	66.63	1	66.63	2.88	0.1205
Residual	231.23	10	23.12		
Lack of Fit	135.23	5	27.05	1.41	0.3580
Pure Error	96.00	5	19.20		
Cor Total	444.95	19			

The Model's "Model F-value" of 1.03 indicates that it is not dangerous significant compared to the noise. A "Model F-value" from that bulk has a 47.95 per cent opportunity of in processed due to noise. Model terms are dangerous signs if the "Prob > F" value is less than 0.0500. There are no important model terms in this situation as shown in Figure 5.

Typical terms are not important in this case. Values o.1000 indicate that the model conditions are not important. Reducing the model may improve it, and therefore many of

the model terms mentioned above are unimportant (not including the terms required for hierarchy attribution and support). The "Lack of Fit F-value" of 1.41 indicates that the lack of fit has no bearing on the pure error. Due to noise, there is a 35.80% possibility that a "Lack of Fit F-value" this arge will occur. It's fine if there's a minor mismatch. As indicated in Table 4 and Table 5 are examples of where we want the Model to fit. "Adeq Precision" determines the signal-to-noise ratio, as shown in Table 6. It's preferable to

have a ratio of more than four. A signal with a ratio of 4.147 is acceptable. This Model can help you find your way around the design world.

8. Interpretation

Figure 6 shows how to optimize capitation using catalytic reaction rate data by setting Velocity near the minimum value (98) and force near the maximum value (100). (4 bar). If you raise Velocity while keeping force constant, Yield drops fast from these settings. If you keep the velocity constant while lowering the force, the Yield similarly drops quickly. In both Velocity and force, quadratic effects may be seen on the surface plot as it modifies one factor while keeping the other constant, the response surface curves. A rising ridge is a name for the shape of this surface.

Statistics Report prototypes the diagnostics dependence in the diagnostics node. These proceed to diagnostic plots and plan a progression as explained in the above show. Response one, Force and Transform: None, as shown in Figures 6 and 7.

Table 6.

Diagnostics Case Statistics and *Exceeds limits

Standard Order	Actual Value	Predicted Value	Residual	Leverage	Internally Studentized Residual	Externally Studentized Residual	Influence on Fitted Value Dffits	Cook's Distance	Run Order
1	30.00	33.09	-3.09	0.670	-1.117	-1.132	-1.612	0.253	17
2	21.00	23.29	-2.29	0.670	-0.829	-0.815	-1.160	0.139	4
3	26.00	27.01	-1.01	0.670	-0.365	-0.349	-0.497	0.027	14
4	26.00	23.21	2.79	0.670	1.008	1.009	1.437	0.206	11
5	24.00	29.57	-5.57	0.670	-2.016	-2.482	* -3.54	0.824	3
6	25.00	26.78	-1.78	0.670	-0.643	-0.623	-0.887	0.084	2
7	25.00	25.49	-0.49	0.670	-0.179	-0.170	-0.242	0.006	13
8	29.00	28.70	0.30	0.670	0.109	0.103	0.147	0.002	5
9	40.00	35.30	4.70	0.607	1.559	1.700	* 2.11	0.376	20
10	29.00	29.76	-0.76	0.607	-0.252	-0.240	-0.299	0.010	7
11	35.00	28.78	6.22	0.607	2.065	2.587	* 3.22	0.659	18
12	23.00	25.28	-2.28	0.607	-0.758	-0.741	-0.921	0.089	10
13	22.00	21.20	0.80	0.607	0.265	0.252	0.313	0.011	6
14	26.00	22.86	3.14	0.607	1.042	1.047	1.302	0.168	16
15	24.00	28.11	-4.11	0.166	-0.937	-0.930	-0.416	0.018	12
16	29.00	28.11	0.89	0.166	0.202	0.192	0.086	0.001	9
17	27.00	28.11	-1.11	0.166	-0.253	-0.241	-0.108	0.001	15
18	23.00	28.11	-5.11	0.166	-1.164	-1.188	-0.531	0.027	8
19	35.00	28.11	6.89	0.166	1.569	1.714	0.766	0.049	19
20	30.00	28.11	1.89	0.166	0.430	0.412	0.184	0.004	1

9. Optimization choices

There are many options for improving and choosing the ideal Model in this research experiment, then choosing the best one based on good results. They are set goals for each Response and numerical optimization conditions to generate solutions that result in optimal force pressure damping. For example, graphical optimization can set minimum or maximum limits for each answer; then, proportionate selections are made to build an overlay graph highlighting an operability portability area. The level of resistance of this spring Cabbage damper (dia. 7 mm) to shocks on the road is determined by the impact of the damping on the compressive force resistance, as shown in Table 6, Figures 7 and 8.

Table 7 and Figure 9. The ideal point that enters the required, ideal operating conditions were predicted using the expected response values of the spring damping operating circumstances in the stiff bikes on rough roads with numerous hazards. As a result, through this design with confidence intervals, we attempted to develop and create a shock absorber that functions in the worst possible ways.

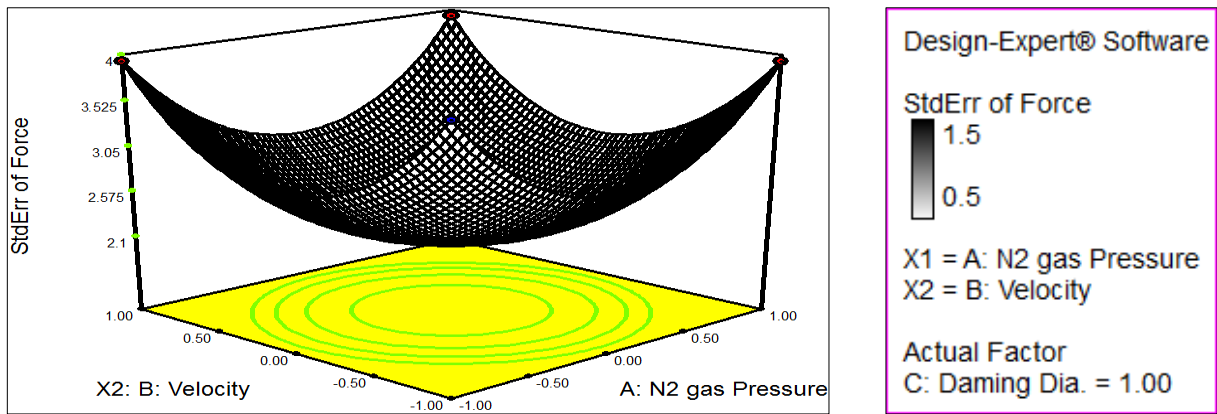


Fig. 6. Relationship between Velocity, gas pressure, and stdErr of force

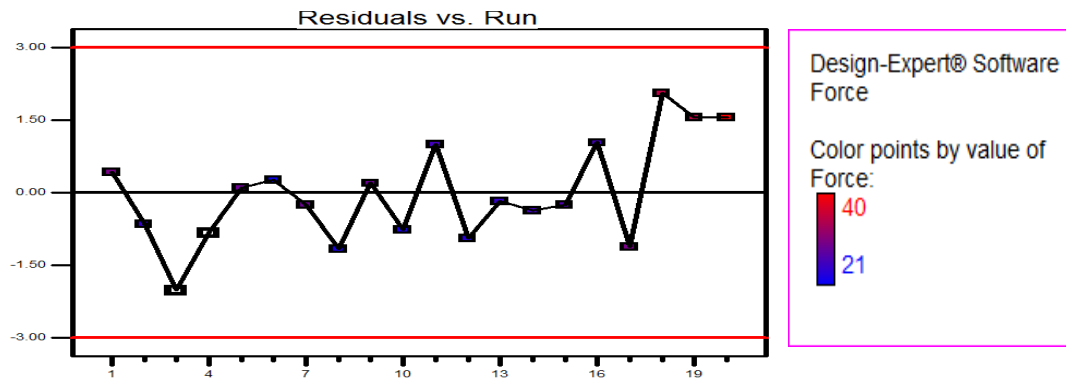


Fig. 7. value force and Residuals VS Run

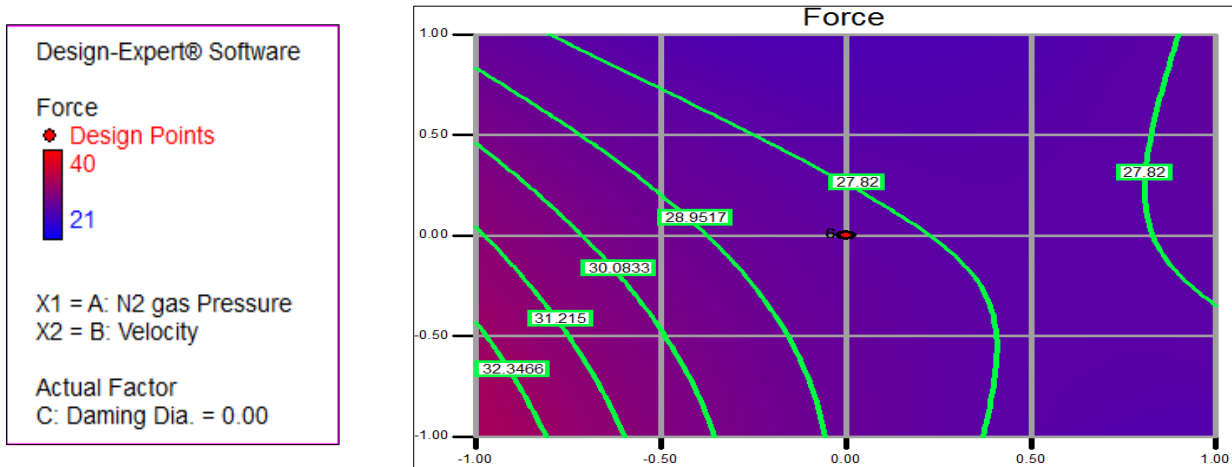


Fig. 8. X1: A: N₂ gas Pressure and X2: B: Velocity

Table 7.
Response prediction

Response	Prediction	SE Mean	95% CI low	95% CI high	SE Pred	95% PI low	95% PI high
Force	33.0856	3.94	24.32	41.85	6.21	19.24	46.93

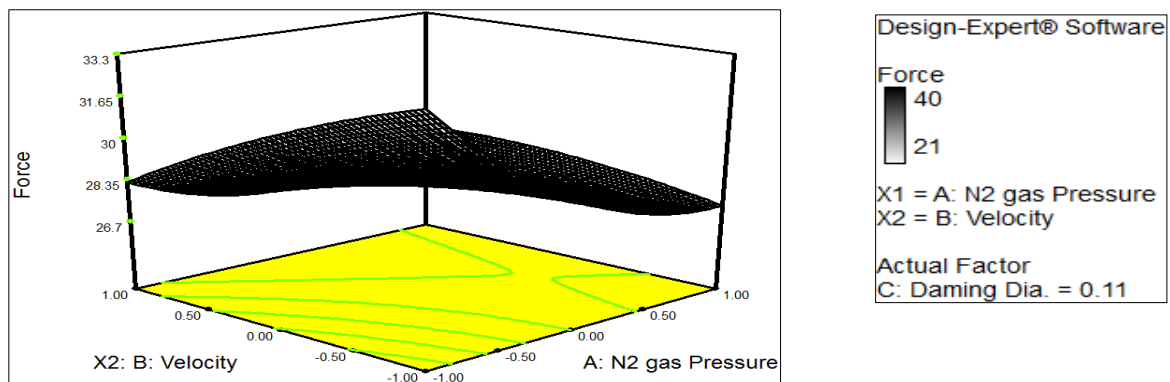


Fig. 9. N2 gas pressure VS Velocity and damping

10. Conclusions

The surface roughness approach was used to identify an optimal setting of the damping force parameters process. Therefore, through the experiment in the laboratory, a set of tests was conducted on the springs and shock absorbers that were applied to a motor vehicle loaded with loads and on unpaved roads at different speeds and loads. The tire cycle is in unpaved roads and has many pitfalls, so we worked to improve and find a shock absorber that works in the worst ways through this design, as shown in Tables 1-7, and Figures 1-9, where the ideal strength Force was 33.0856, stander error 3.94, Individual 95% CI low for mean based on pooled StDev 24.32, Individual 95% CI high 41.85, SE Pred 6.21, 95% PI low 19.24 and 95% PI high 46.93. N2 gas pressure (30,35,40 bar), Damping Dia. (1,1.6,1.9 mm), and Suspension velocity (0.7,0.8,0.1 m/s) were selected as process parameters for the experimental plan using the Central Composite Design.

The results of the ideal levels of damping force process parameters for optimum damping force are such follows:

1. The three main factors most influencing where the diameter of the spring damping, followed by its resistance to the compressive force during shocks (bumps) in the unpaved roads through laboratory experiments.
2. It has found the best level in laboratory operating parameters through a group of operations, and they were in Table 6 and Table 7.
3. And the predictive results were identical to the results experimental laboratory.
4. Confirmed results to good agreement with the prediction made by regression analysis.

References

- [1] Z. Zeng, X. Huang, Z. Li, W. Wang, Z. Shi, Y. Yuan, A.A. Shuaibu, Experimental Research on Vibration-

Damping Effect of Combined Shear Hinge Prefabricated Steel Spring Floating Slab Track, Sensors 22/7 (2022) 2567.

DOI: <https://doi.org/10.3390/s22072567>

- [2] W.H. Tan, W.C. Lo, C.Y. Teoh, E.M. Cheng, Structural Analysis on the Coil Spring of Motorcycle Suspension System, Journal of Physics: Conference Series 2051 (2021) 012031. DOI: <https://doi.org/10.1088/1742-6596/2051/1/012031>
- [3] A. Dobre, Modelling the dynamic behaviour of car hydraulic dampers, IOP Conference Series: Materials Science and Engineering 1091 (2021) 012018. DOI: <https://doi.org/10.1088/1757-899X/1091/1/012018>
- [4] D.C. Montgomery, Design and Analysis of Experiments, Wiley, Hoboken, 2012.
- [5] Performance: Damping Technology by ZF. Available from: https://www.zf.com/master/media/en/corporate/m_zf.com/company/download_center/products/passenger_cars/2019_09_13_zf_dampingtechnology.pdf
- [6] A. Dębowski, Analysis of the Effect of Mass Parameters on Motorcycle Vibration and Stability, Energies 14/16 (2021) 5090. DOI: <https://doi.org/10.3390/en14165090>
- [7] M.D. Rao, S. Gruenberg, Measurement of Equivalent Stiffness and Damping of Shock Absorber, Experimental Techniques 26/2 (2002) 39-42. DOI: <https://doi.org/10.1111/j.1747-1567.2002.tb00061.x>
- [8] A.Y. Ismail, Al Munawwir, A. Pamungkas, Stiffness-based Spring Design Optimization using Taguchi Method to reduce Low-Frequency Vibration, Jurnal Mekanova 5/2 (2019) 57-65. DOI: <https://doi.org/10.35308/jmkn.v5i2.1635>
- [9] M.G. Elankovan, A. Sai Ramesh, Conceptual Design of Electromagnetic Damper for Motorcycle Suspension System, International Journal of Engineering Research and Technology 4/08 (2015) 472-476. DOI: <https://doi.org/10.17577/IJERTV4IS080580>

- [10] G. Taguchi, S. Konishi, Taguchi methods, orthogonal arrays and linear graphs, tools for quality engineering, American Supplier Institute, Dearborn, 1987, 8-35.
- [11] G. Taguchi, Introduction to quality engineering, McGraw-Hill, New York, 1990.
- [12] M. Holm, Development and construction of a mechanically sprung shock absorber with adjustable spring stiffness for mountain bikes, MSc Thesis, KTH, Stockholm, Sweden, 2021.
- [13] M.I. Al-Maliki Saifudin, N.M. Usamah, Z.M. Ripin, Attenuation of motorcycle handle vibration using dynamic vibration absorber, MATEC Web of Conferences 217 (2018) 01006.
DOI: <https://doi.org/10.1051/mateconf/201821701006>
- [14] M. Sreenivasan, M. Dinesh Kumar, R. Krishna, T. Mohanraj, G. Suresh, D. Hemanth Kumar, A. Sai Charan, Finite element analysis of coil spring of a motorcycle suspension system using different fibre materials, Materials Today: Proceedings 33/1 (2020) 275-279.
DOI: <https://doi.org/10.1016/j.matpr.2020.04.051>
- [15] R.A. Johnson, C.B.Gupta, Probability and Statics for Engineers, Pearson Education, India, 2006.
- [16] D. Dabrowski, W. Cioch, Analysis of signals pre-processing algorithm in case of hardware and software implementation on diagnostic programmable device PUD-2, Acta Physica Polonica A 123/6 (2013) 1020-1023.
- [17] A. Chinnamahammad Bhasha, N. Vijay Rami Reddy, B. Rajnaveen, Design And Analysis of Shock Absorber, International Research Journal of Engineering and Technology 04/01 (2017) 201-207.
- [18] M. Othmani, K. Zarbane, A. Chouaf, Effect of infill and density pattern on the mechanical behaviour of ABS parts manufactured by FDM using Taguchi and ANOVA approach, Archives of Materials Science and Engineering 111/2 (2021) 66-77.
DOI: <https://doi.org/10.5604/01.3001.0015.5806>
- [19] A. El Magri, S. Vaudreuil, Optimizing the mechanical properties of 3D-printed PLA-graphene composite using response surface methodology, Archives of Materials Science and Engineering 112/1 (2021) 13-22.
DOI: <https://doi.org/10.5604/01.3001.0015.5928>
- [20] H.K. Hasan, Analysis of the effecting parameters on laser cutting process by using response surface methodology (RSM) method, Journal of Achievements in Materials and Manufacturing Engineering 110/2 (2022) 59-66.
DOI: <https://doi.org/10.5604/01.3001.0015.7044>
- [21] H.M. Magid, Experimental study of mild steel cutting process by using the plasma arc method, Journal of Achievements in Materials and Manufacturing Engineering 108/2 (2021) 75-85.
DOI: <https://doi.org/10.5604/01.3001.0015.5066>
- [22] S. Adeeb, S. Adeeb, G. Chladek, W. Pakieła, A. Mertas, Influence of silver-containing filler on antibacterial properties of experimental resin composites against Enterococcus faecalis, Journal of Achievements in Materials and Manufacturing Engineering 109/2 (2021) 59-67.
DOI: <https://doi.org/10.5604/01.3001.0015.6259>
- [23] M. Czerwiński, J. Żmudzki, K. Kwieciński, M. Kowalczyk, Finite element analysis of the impact of the properties of dental wedge materials on functional features, Archives of Materials Science and Engineering 112/1 (2021) 32-41.
DOI: <https://doi.org/10.5604/01.3001.0015.5930>
- [24] O. Aourik, M. Othmani, B. Saadouki, Kh. Abouzaid, A. Chouaf, Fracture toughness of ABS additively manufactured by FDM process, Journal of Achievements in Materials and Manufacturing Engineering 109/2 (2021) 49-58.
DOI: <https://doi.org/10.5604/01.3001.0015.6258>



© 2022 by the authors. Licensee International OCSCO World Press, Gliwice, Poland. This paper is an open access paper distributed under the terms and conditions of the Creative Commons Attribution-NonCommercial-NoDerivatives 4.0 International (CC BY-NC-ND 4.0) license (<https://creativecommons.org/licenses/by-nc-nd/4.0/deed.en>).